Lovejoy, S., B. Watson, D. Schertzer, G. Brosamlen, 1995: Scattering in multifractal media. Proc. of Particle Transport in Stochastic Media. L. Briggs Ed., American Nuclear Society, Portland, Or., 750-760, April 30-May 4 1995.

SCATTERING IN MULTIFRACTAL MEDIA:

Shaun Lovejoy, Physics Department, McGill University, 3600 University st., Montreal, Que. H3A 2T8, CANADA

Brian Watson, Physics dept., St. Lawrence University, Canton, N.Y. 13617, USA

Daniel Schertzer, L. M. D., U. P. et M. Curie, Tour 15-25, BP 99, 4 Pl. Jussieu, Paris 75005, FRANCE

Gerd Brosamlen, Physics Department, McGill University, 3600 University st., Montreal, Que. H3A 2T8, CANADA

ABSTRACT:

We develop a formalism for particle/photon scattering statistics in media ("clouds") whose density is a multifractal measure. The basic quantities are the size of the medium measured in units of mean free paths (κ), the codimension function of the media density and scattering analogue codimension function. We obtain simple relations asymptotic in κ between these functions and hence obtain the single scattering statistics. We suggest a way to renormalize the multifractal so as to obtain an equivalent homogeneous medium, and we estimate anomalous diffusion exponents. Numerical simulations show that the results are very accurate even when κ is not large.

1. INTRODUCTION

Geophysical systems such as the atmosphere exhibit extreme variability over ranges of scale which can exceed factors of 10^9. The simplest dynamical models of these systems are scale invariant; indeed, a growing body of theoretical and empirical work is showing that geophysical systems do indeed obey scaling symmetries over considerable ranges (for reviews, see [1], see also papers in [2-4]. Growing recognition of this has lead to mushrooming interest in scaling models of a wide variety of geophysical systems. In particular, thanks to advances in scaling ideas - particularly multifractals and generalized scale invariance - models can now be sufficiently realistic that they can be used for simulating various physical processes including transport phenomena. In the following, for convenience we consider our media to be a cloud, and the particles, photons, although applications involving neutrons in turbulent media suggest themselves.

Starting with [5], fractal models of clouds have been used to numerically study the radiative properties of extremely variable clouds. Note that unlike Markovian random media, multifractals have long range algebraic rather than short range exponential decorrelations. Techniques for studying the transfer on the latter (e.g. [6]) would not appear to be appropriate. Since then they have been used in a series of papers [7-11] who used simple fractal ("β") models to investigate the "bulk" properties (overall mean albedo and transmittance) of clouds. Many other researchers [12-14] have now used fractal or multifractal cloud models for modeling radiative transport, although most results so far have been numerically derived and the all important effective optical thickness has been quite low (typically <3, i.e. below the thick cloud regime). References [15-16] was the first to go beyond "bulk" flux estimates by numerically calculating detailed radiation fields. This was done on large (1024x1024) two dimensional multifractal cloud models using a class of universal multifractals (lognormals). Below, we will theoretically derive one of the key numerical results of this study; the bulk transmittance exponent.

While numerical approaches (which are nontrivial for multifractals) certainly provide indispensable tools for understanding radiation in scaling systems, in themselves they are insufficient to resolve the two basic physical problems: the statistical relationship between the radiation and cloud fields (as functions of resolution), and the scattering statistics describing the random trajectories of individual photons. While the above references contain some first steps in theoretically addressing the former, references [8, 15] have obtained some initial results concerning the latter. Unfortunately, while their results (mostly direct transmittance statistics) apply to arbitrary multifractal clouds, they are only valid in the asymptotic limit involving small distances. In this paper[a] we obtain much more useful results asymptotic in the log of the optical thickness. Elsewhere, we extend these results to give a fuller treatment of multiple scattering and a more complete treatment of universal multifractals. Many results are exact for all optical thicknesses and even the asymptotic thick cloud regime turns out to be attained for quite low thicknesses (in the range 4-10) hence our results are widely applicable. We also use our results to renormalize the multifractal; effectively reducing the multifractal transfer problem to a standard homogenous transfer problem but with a drastically reduced "effective" extinction coefficient. Finally, we show how this result can be understood in the context of some recent results on diffusion in multifractals.

[a]The basic framework was announced in [36].

2. BASIC THEORY

2.1 MULTIFRACTAL CLOUDS:

The multifractal models considered here were first developed as phenomenological models of turbulent cascades. In hydrodynamic turbulence, the governing nonlinear dynamical (Navier-Stokes) equations have three basic properties that lead to the cascade phenomenology: 1) scaling symmetry , 2) a quantity conserved by the cascade (energy fluxes from large to small scale), and 3) localness in Fourier space (i.e. the dynamics are most effective between neighboring scales). Cascade models are relevant in the atmosphere and in particular in clouds since the underlying dynamics is of hydrodynamic turbulent origin. There is now a whole series of such phenomenological models: the "pulse-in-pulse" model [17], the lognormal model [18-20], the weighted-curdling model [21], the β-model [22], the α-model [23], the random β-model [24], the p-model [25], and the continuous universal cascade models [26-27].

In cascade processes, a large structure of characteristic length =L and density ρ (initially constant=1) is broken up into smaller substructures of characteristic length $l = L/\lambda$. The density in each substructure is multiplicatively modulated by a random factor (keeping the overall ensemble average fixed $<\rho_\lambda>=1$). When this process is repeated (the overall ratio λ is increased) larger and larger values of ρ_λ appear, concentrated on smaller and smaller scales. The overall result is highly intermittent with the property [27]:

$$\Pr(\rho_\lambda \geq \lambda^\gamma) \approx \lambda^{-c(\gamma)} \tag{1}$$

(equality is within slowly varying functions of λ such as logarithms). The codimension function c(γ) is a statistical scaling exponent characterizing the probability distribution. γ is an order of singularity since it specifies the rate that ρ_λ diverges as $\lambda\rightarrow\infty$. When the dimension of the embedding space D > c(γ) it is simply the fractal codimension of the set of density measures ρ_λ exceeding the threshold λ^γ .

The other equivalent approach to describe the multifractal field is to specify the scaling of the statistical moments $<\rho_\lambda^q>$. We define the multiple-scaling exponent K(q):

$$<\rho_\lambda^q>=\lambda^{K(q)}=\int_{-\infty}^{\infty}\lambda^{q\gamma}p(\gamma,\lambda)d\gamma\,, \qquad \lambda>1 \tag{2}$$

with p(γ,λ)=dPr/dγ is the probability density of γ as a function of λ. The moment exponent K(q) is related to the scaling exponent c(γ) by the following Legendre transformation [28]:

$$K(q)=\max_\gamma[q\gamma-c(\gamma)]$$

$$c(\gamma)=\max_q[q\gamma-K(q)] \tag{3}$$

hence, we obtain a one to one relation between singularities and moments: q=c'(γ), γ=K'(q).

If no further information is available, to fully characterize the process, the entire K(q) or c(γ) function will be required. This is equivalent to an infinite number of parameters; modelling and analysis would be unmanageable. Fortunately, as is often the case in physics, the dynamical cascade processes possess stable and attractive generators leading to "universal multifractals" [27]; for conserved (stationary) processes, the latter can be characterized by only two parameters (α, C_1) (see eq. 4). These have relatively straightforward physical interpretations: respectively, the degree of multifractality, the sparseness of the field . The primary parameter α (the Levy index of the generator) is bounded below by 0 corresponding to the monomfractal minimum, and above at 2, the lognormal multifractal.

$$c(\gamma)=C_1\left(\frac{\gamma}{\alpha' C_1}+\frac{1}{\alpha}\right)^{\alpha'} \qquad \frac{1}{\alpha}+\frac{1}{\alpha'}=1 \tag{4}$$

$$K(q)=\frac{C_1}{\alpha-1}(q^\alpha-q)$$

When α<2, the above is valid for q≥0; otherwise it =∞; we have negative temperature "multifractal phase transitions"[b]. For 1<α<2, c(γ)=0 for $\gamma<-(C_1/(\alpha-1))$; the slowly varying factors in eq. 1 dominate corresponding to frequent low density "Levy holes". For 0≤α<1, $\gamma<C_1/(1-\alpha)$. Below we will illustrate our ideas primarily conserved lognormal multifractals.

2.2 PARTICLE SCATTER/ RADIATIVE TRANSFER:

---

[b]The terminology is due to the existence of a formal analogy between multifractals and classical thermodynamics.

Here we outline recent results which provide the basis for systematic study of radiative transport in multifractal media. Specifically, we indicate how formulae analogous to eqs. 2, 3 for the multifractal optical density field arise for radiative properties. Consider the following definitions:

k= extinction coefficient [m^2Kg^{-1}]
$\langle\rho\rangle$ = mean cloud density [kgm^{-3}]
l = random photon path distance [m]
L= size of cloud [m]
l_m= mean free path (m.f.p.) of a photon in the equivalent homogeneous cloud =$(k\langle\rho\rangle)^{-1}$ [m]
$\lambda=L/l$ = scale ratio $\leq \Lambda$, (Λ=maximum cascade resolution)
$x=l/L=\lambda^{-1}$ random photon nondimensional distance, (fraction of cloud)
$\tau_p = l/l_m$ = random photon distance, (no. of homogeneous cloud m.f.p.'s = kx)
$\kappa = L/l_m$ = extinction parameter = no. of m.f.p.'s across cloud = mean optical depth = extinction coefficient in units such that L=1, $\langle\rho\rangle$=1.

The optical distance over a physical distance l is thus:

$$\tau(l) = \int_l k\rho_\Lambda(z)dz = k\rho_{l,d}l \quad (5)$$

where we have written $\rho_{l,d}$ for the average dressed density at resolution l. In multifractal theory it is important to distinguish between the "bare" and the "dressed" quantities [27]. The bare quantity is obtained after the cascade generating the cloud field, has proceeded down to scale λ. The corresponding dressed quantity however is obtained after integrating the completed cascade over the same scale. This implies that the bare quantities have no small scale interactions, whereas the dressed ones have a full range of interactions. A cascade whose development is limited to the scale Λ is "bare" on this scale: no smaller activity is hidden or "dressed". The difference arises for high order moments $\langle \tau_d^q \rangle \to \infty$ for $q > q_D$, where q_D is the solution of $K(q_D) = (q_D - 1)D$, where D (=1 in eq. 5) is the dimension of the averaging set (see [27]). This result can be understood as the fact that -with the exception of rare violent flucuations - the spatial integration smooths out all the "hidden" small scale fluctuations. This implies the approximate equivalence of the bare and dressed for all but the strongest fluctuations; fortunately, we shall see that the corresponding high density regions are unimportant for the transfer.

Using the above notation with the bare=dressed approximation $\rho_{\lambda,d} = \rho_\lambda$, we obtain:

$$\tau(\gamma,\lambda) = \frac{\rho_\lambda}{\langle\rho\rangle}\lambda^{-1}\frac{L}{l_m} = \lambda^{\gamma-1}\kappa \quad (6)$$

which is the optical thickness over a distance l through a singularity of order γ. The direct (unscattered) transmission T across this distance is thus:

$$T(l) = e^{-\tau(l)} \quad (7)$$

Since the transmittance is the probability distribution for photon path lengths, we can average over the singularities and obtain:

$$\Pr(l' > l) = \langle T(l) \rangle = \langle e^{-\tau(l)} \rangle \quad (8)$$

Take τ_p as the dimensionless photon path and write it as a scaling function with an order of singularity γ_p defined as follows:

$$\tau_p = \kappa^{\gamma_p} = \frac{l}{l_m} = \kappa x = \kappa\lambda^{-1} \quad (9)$$

or:

$$\lambda = \kappa^{(1-\gamma_p)} \quad (10)$$

since $\lambda>1$, $\kappa>1$, we have $\gamma_p \leq 1$; also $\Lambda > \kappa^{1-\gamma_p}$.

We can now obtain a multifractal scattering formalism in which the extinction coefficient κ takes the place of the scaling parameter λ. Instead of the codimension function $c(\gamma)$ of the singularities of the cloud density γ we rather talk about an analogue codimension function $c_p(\gamma_p)$ which describes how the single photon path distance singularity γ_p varies with the extinction coefficient:

$$\Pr(\tau_p \geq \kappa^{\gamma_p}) = \Pr(l' > l) \approx \kappa^{-c_p(\gamma_p)} \quad (11)$$

2. BASIC THEORY

2.1 MULTIFRACTAL CLOUDS:

The multifractal models considered here were first developed as phenomenological models of turbulent cascades. In hydrodynamic turbulence, the governing nonlinear dynamical (Navier-Stokes) equations have three basic properties that lead to the cascade phenomenology: 1) scaling symmetry , 2) a quantity conserved by the cascade (energy fluxes from large to small scale), and 3) localness in Fourier space (i.e. the dynamics are most effective between neighboring scales). Cascade models are relevant in the atmosphere and in particular in clouds since the underlying dynamics is of hydrodynamic turbulent origin. There is now a whole series of such phenomenological models: the "pulse-in-pulse" model [17], the lognormal model [18-20], the weighted-curdling model [21], the β-model [22], the α-model [23], the random β-model [24], the p-model [25], and the continuous universal cascade models [26-27].

In cascade processes, a large structure of characteristic length =L and density ρ (initially constant=1) is broken up into smaller substructures of characteristic length $l = L/\lambda$. The density in each substructure is multiplicatively modulated by a random factor (keeping the overall ensemble average fixed $<\rho_\lambda>= 1$). When this process is repeated (the overall ratio λ is increased) larger and larger values of ρ_λ appear, concentrated on smaller and smaller scales. The overall result is highly intermittent with the property [27]:

$$\Pr(\rho_\lambda \geq \lambda^\gamma) \approx \lambda^{-c(\gamma)} \tag{1}$$

(equality is within slowly varying functions of λ such as logarithms). The codimension function c(γ) is a statistical scaling exponent characterizing the probability distribution. γ is an order of singularity since it specifies the rate that ρ_λ diverges as $\lambda \to \infty$. When the dimension of the embedding space D > c(γ) it is simply the fractal codimension of the set of density measures ρ_λ exceeding the threshold λ^γ .

The other equivalent approach to describe the multifractal field is to specify the scaling of the statistical moments $<\rho_\lambda^q>$. We define the multiple-scaling exponent K(q):

$$<\rho_\lambda^q>=\lambda^{K(q)}=\int_{-\infty}^{\infty}\lambda^{q\gamma}p(\gamma,\lambda)d\gamma, \quad \lambda>1 \tag{2}$$

with p(γ,λ)=dPr/dγ is the probability density of γ as a function of λ. The moment exponent K(q) is related to the scaling exponent c(γ) by the following Legendre transformation [28]:

$$K(q)=\max_\gamma[q\gamma-c(\gamma)]$$

$$c(\gamma)=\max_q[q\gamma-K(q)] \tag{3}$$

hence, we obtain a one to one relation between singularities and moments: q=c'(γ), γ=K'(q).

If no further information is available, to fully characterize the process, the entire K(q) or c(γ) function will be required. This is equivalent to an infinite number of parameters; modelling and analysis would be unmanageable. Fortunately, as is often the case in physics, the dynamical cascade processes possess stable and attractive generators leading to "universal multifractals" [27]; for conserved (stationary) processes, the latter can be characterized by only two parameters (α, C_1) (see eq. 4). These have relatively straightforward physical interpretations: respectively, the degree of multifractality, the sparseness of the field . The primary parameter α (the Levy index of the generator) is bounded below by 0 corresponding to the monomfractal minimum, and above at 2, the lognormal multifractal.

$$c(\gamma)=C_1\left(\frac{\gamma}{\alpha' C_1}+\frac{1}{\alpha}\right)^{\alpha'} \qquad \frac{1}{\alpha}+\frac{1}{\alpha'}=1 \tag{4}$$

$$K(q)=\frac{C_1}{\alpha-1}(q^\alpha-q)$$

When α<2, the above is valid for q≥0; otherwise it =∞; we have negative temperature "multifractal phase transitions"[b]. For 1<α<2, c(γ)=0 for $\gamma<-(C_1/(\alpha-1))$; the slowly varying factors in eq. 1 dominate corresponding to frequent low density "Levy holes". For 0≤α<1, $\gamma<C_1/(1-\alpha)$. Below we will illustrate our ideas primarily conserved lognormal multifractals.

2.2 PARTICLE SCATTER/ RADIATIVE TRANSFER:

---

[b]The terminology is due to the existence of a formal analogy between multifractals and classical thermodynamics.

$$\langle \tau_p^{q_p} \rangle = f_p(q_p)\kappa^{K_p(q_p)} \tag{12}$$

$f_p(q_p)$ is the prefactor which is given explicity since we will calculate it below. c_p, K_p will be linked by a Legendre transform as in the standard multifractal case.

The mean transmission in eq. 8 is obtained by averaging over the singularities, using eq. 2 to obtain the probability density of γ:

$$\langle T(\gamma,\lambda)\rangle = \int_{-\infty}^{\infty} e^{-\tau(\gamma,\lambda)} p(\gamma,\lambda)d\gamma \tag{13}$$

From eq. 2 we see that $\lambda^{K(q)}$ is the (base λ, bilateral) Laplace transform of the probability density. It will turn out to be convenient to write the probability density $p(\gamma,\lambda)$ in terms of its inverse Laplace transform:

$$p(\gamma,\lambda) = \frac{\log\lambda}{2\pi i}\int_{c-i\infty}^{c+i\infty} \lambda^{K(q)-q\gamma} dq \tag{14}$$

where c is chosen so that the path of integration passes to the left of the poles in the complex q plane. We now use the following transformation of variables:

$$1-\gamma = \frac{1-\gamma_\tau}{1-\gamma_p} \tag{15}$$

to replace the integration over γ by one over γ_τ:

$$\langle T(\gamma_p,\kappa)\rangle = \frac{1}{2\pi i}\int_{c-i\infty}^{c+i\infty} \kappa^{q\gamma_p+(1-\gamma_p)K(q)} \int_{-\infty}^{\infty} e^{-\kappa^{\gamma_\tau}-q\gamma_\tau\log\kappa} d(\gamma_\tau \log\kappa) dq \tag{16}$$

We now use the following:

$$\int_{\gamma_{pmin}}^{\infty} e^{-\kappa^{\gamma_\tau}-q\gamma_\tau\log\kappa} d(\gamma_\tau\log\kappa)dq = \Gamma\left(-q,\kappa^{\gamma_{pmin}}\right) \approx \frac{1}{q}\kappa^{-q\gamma_{pmin}} + \Gamma(-q) \tag{17}$$

valid for all q, the far right approximation is valid for a lower cutoff $\gamma_{pmin} \ll 0$. Hence for $q \le 0$ we can take the limit $\gamma_m \to -\infty$ and obtain:

$$\Pr\left(\tau_p > \kappa^{\gamma_p}\right) \approx \kappa^{-c_p(\gamma_p)} = \langle T(\gamma_p,\kappa)\rangle = \frac{1}{2\pi i}\int_{c-i\infty}^{c+i\infty} \kappa^{q\gamma_p+(1-\gamma_p)K(q)}\Gamma(-q)dq \tag{18}$$

note that $\Gamma(-q)$ has a simple pole at 0 and at positive integers, hence the contour in the above integral must pass to the left of the origin in the complex q plane. In order to extend the region of analyticity (and hence of validity of the results below), we may consider the probability density, obtained by differentiating eq. 17 with respect to γ_p:

$$p(\gamma_p) = \frac{1}{2\pi i}\int_{c-i\infty}^{c+i\infty} (-q+K(q))\Gamma(-q)\kappa^{q\gamma_p+(1-\gamma_p)K(q)}dq \tag{19}$$

The extension of the above formula for $q<1$ (rather than $q<0$) is usually possible since the rapidly oscillating term $q^{-1}\kappa^{-q\gamma_{pmin}}$ (eq. 17) usually gives no contribution. For example, consider the case where $\alpha=2$ or $K(q)$ is nonuniversal but analytic for $\mathrm{Re}(q)<1$. Here this oscillating term has a saddle point at a value q given by $K'(q) = -(\gamma_p-\gamma_m)/(1-\gamma_p) \to -\infty$; however the corresponding value of the exponent is $-c(-\infty)(1-\gamma_p)<0$ so that the contribution is negligeable for large κ. It turns out that it can be also be neglected for universal multifractals with $\alpha>1$, although for $\alpha<1$, there is no convergence.

Now, introduce the following change of variables:

$$q_p = K(q) - q \tag{20}$$

This transformation is 1-1 as long as $0>\mathrm{Re}(q_p)>\min(K(q)-q)=-c(1)$; so that the above relation will be analytic and single valued. Note the particular value $q(-1)=1$. Also, since $\Gamma(-q)$ has a pole at q=1, the following will be valid for $q_p>-1$ (the transformation will be single valued since for $C_1<1$, $c(1)>1$).

$$p(\gamma_p) = \frac{1}{2\pi i}\int_{c-i\infty}^{c+i\infty}\left(\left(K(q(q_p))-q(q_p)\right)\Gamma(-q(q_p))\frac{dq}{dq_p}\right)\kappa^{K(q(q_p))}\kappa^{-\gamma_p q_p}dq_p = \frac{\log\kappa}{2\pi i}\int_{c-i\infty}^{c+i\infty} f_p(q_p)\kappa^{K_p(q_p)}\kappa^{-q_p\gamma_p}dq_p \tag{21}$$

The corresponding integration contour for q_p can be deformed into a line parallel to the imaginary axis, offset by the small amount c (<0 here). The limits of integration have been deformed appropriately, by taking advantage of the analyticity of the integrand in the negative real half-plane (avoiding poles, and in the case $\alpha<2$, the branch point at the origin). The far right equality is the inverse Laplace transform (corresponding to eq. 14). By inspection, we obtain:

$$K_p(q_p) = K(q(q_p)) = q_p + q(q_p)$$

$$f_p(q_p) = \frac{q_p \Gamma(-q(q_p))}{1 - K'(q(q_p))} (\log \kappa)^{-1} \tag{22}$$

with q, q_p related by eq. 22.

We can now calculate $c_p(\gamma_p)$ using the saddle point method on eq. 18, we obtain:

$$c_p(\gamma_p) = -\min_q \left(q\gamma_p + (1-\gamma_p)K(q)\right) = (1-\gamma_p)\, c\left(\frac{-\gamma_p}{1-\gamma_p}\right)$$

$$f_p(\gamma_p) \approx f_p\left(c'\left(\frac{-\gamma_p}{1-\gamma_p}\right)\right) \tag{23}$$

The above is valid for multifractals with K(q) analytic for $q=c'(\gamma)<1$ (if universal, then for $\alpha=2$ only, when $1<\alpha<2$ only for small γ_p; see [29]). The minimization condition determining the saddle point is the usual $K'(q)=\gamma$ where:

$$\gamma = \frac{-\gamma_p}{(1-\gamma_p)} \tag{24}$$

Under the above conditions, we obtain two families of codimension and moment scaling functions; their mutual relations are given in table 2.

Photon statistics	Cloud statistics
q_p	$=-q+K(q)$
$K_p(q_p) = \max_{\gamma_p}[q_p\gamma_p - c_p(\gamma_p)]$	$=K(q) = \max_\gamma [q\gamma - c(\gamma)]$
$1-\gamma_p$	$=1/(1-\gamma)$
$c_p(\gamma_p) = \max_q [q\gamma_p - K_p(q_p)]$	$\frac{c(\gamma)}{1-\gamma} = \frac{\max_q[q\gamma - K(q)]}{1-\gamma}$

Table 1: Summary of relations between multifractal cloud and photon scattering exponents.

To give an example of the above, consider the $\alpha=2$ (lognormal multifractal). We have:

$$c(\gamma) = C_1\left(\frac{\gamma}{C_1}+1\right)^2 \qquad c_p(\gamma_p) = \frac{\left(1-(1+C_1)(1-\gamma_p)\right)^2}{4C_1(1-\gamma_p)}$$

$$K(q) = C_1(q^2 - q) \qquad K_p(q_p) = q_p - \frac{\sqrt{(1+C_1)^2 + 4C_1 q_p} - (1+C_1)}{2C_1} \tag{25}$$

Numerics have shown (see below and [30]) that formulae (23) are accurate even for clouds with mean optical thickness as low as 4-10 (formulae 22 -when applicable- are exact).

2.3 Probability density near the most probable path length:

In the thick cloud limit, scattering will be dominated by the most probable scattering. Concentrating on the lognormal case (which will in fact be a good approximation to all cases where K(q) is analytic at q=0) the most probable scattering occurs for q=0, $\gamma=-C_1$, $\gamma_p=C_1/(1+C_1)$ (ignoring the corrections). Using eq. 20 with $\alpha=2$, we obtain for γ_p near enough the minimum:

$$p(\gamma_p) \approx (1+C_1)^{-1} e^{\frac{(1+C_1)\left(\frac{C_1}{(1+C_1)}-\gamma_E\right)^2}{4C_1 \log\kappa}} \kappa^{-\frac{(1+C_1)}{4C_1}\left(C_1-(1+C_1)\gamma_p+\frac{1}{\log\kappa}\left(\gamma_E-\frac{C_1}{1+C_1}\right)\right)^2} \quad (26)$$

i.e. as κ increases, the transport will become dominated by photons traveling a (nondimensional) distance τ_p:

$$\tau_p = \kappa^{\frac{C_1}{1+C_1}} e^{\frac{\left(\gamma_E - \frac{C_1}{1+C_1}\right)}{1+C_1}} \kappa^{\Delta\gamma_p} \quad (27)$$

where $\Delta\gamma_p$ is a normal random variable with $<\Delta\gamma_p>=0$, $<\Delta\gamma_p^2> = 2C_1(1+C_1)^{-1}(\log\kappa)^{-1}$ (i.e. variance decreasing with logκ).

3. NUMERICAL SIMULATIONS AND DRESSED STATISTICS

3.1 SIMULATING THE MULTIFRACTAL CLOUDS

The above calculations were made assuming that for the significant singularities, the bare and dressed densities are equal. The difference is in fact a "hidden" singularity (see [31] for this and the relation to self-organized criticality) which gives rise to an independent factor which modulates the bare statistics. The precise result is that this random factor is of order 1, except for very rare extreme events with $\gamma > \gamma_D = K'(q_D)$ where q_D is defined in section 2; the critical order of divergence. To compare this "bare" approximation we simulate the transport through multifractal fields using a continuous cascade algorithm [27]. Simulations were performed using three C_1 different codimensions of the mean, $C_1=0.1$, $C_1=0.5$, $C_1=0.9$, corresponding to increasingly violent fluctuations in the cloud model. Note that real cloud radiation fields[c] have parameters estimated to be roughly $\alpha \approx 1.35$, $C_1 \approx 0.15$ depending somewhat on the wavelength[d] (see [32]).

3.2 SIMULATING THE TRANSPORT:

For the numerical simulations of the transport we simply discretize the optical depth integral and calculated the ensemble averaged transmission as a function of pathlength $\tau_p=\kappa x$:

$$< T(\tau_p) > = < e^{-\kappa\sum_i \rho_\Lambda(x_i)\Lambda^{-1}} > = < \prod_i e^{-\kappa\rho_\Lambda(x_i)\Lambda^{-1}} > \quad (28)$$

The simulated multifractal cloud density field $\rho_\Lambda(x_i)$ had the resolution (scale of homogeneity) Λ^{-1}, with an overall optical thickness of κ (since $<\rho_\Lambda>=1$ and the external scale=1). To calculate the transmission through one realization the photon starting points inside the cloud were randomly chosen (see fig. 1). Moreover we implemented periodic boundary conditions and calculated the transmission for $0 < \tau_p < \kappa$. Finally the ensemble average was taken over the total number of realizations. This procedure was repeated for increasing extinction coefficients $\kappa = 2^n$; n=1,2,...,10.

The analyzing technique used for the simulated data is the Probability Distribution/Multiple Scaling method (PDMS) ([33-34]). For each fixed order of singularity γ_p the logarithm of the probability distribution is plotted versus the logarithm of κ. If the probability distribution obeys eq. 11, these points lie on a straight line, whose absolute slope is $c_p(\gamma_p)$ (fig. 2). The sub-exponential prefactors determine the intercept. In order to obtain accurate estimates, we analyse the probability distributions rather than densities and determine both probability distributions $\Pr(\tau_p > \kappa^{\gamma_p})$ for the right rising branch of $c_p(\gamma_p)$ and $\Pr(\tau_p < \kappa^{\gamma_p})$ for the left branch. There are two distinct intercepts i.e. different prefactors for either probability distribution which can be seen very well in fig. 2. An advantage of examining the path length distribution this way, is that it includes a range of scales of κ rather then just a single scale thus increasing the accuracy of the estimates. The "dressed" probability distribution exponent $c_{p,d}(\gamma_p)$ obtained this way is compared with the analytically derived[e] $c_p(\gamma_p)$ (fig. 3).

We also checked the scaling of the moments of the dressed photon path length with respect to κ. This is done by plotting $\log < \tau_p^q >$ versus $\log\kappa$ (fig. 4). As previously, the aim is to compare the bare and the dressed statistics. If the dressed moments are scaling (i.e. they obey eq. 12), the points for each specific moment q lie on a straight line, whose slope is $K_{p,d}(q)$. In fig. 5 we compare the "dressed" moment scaling exponent $K_{p,d}(q)$ with the analytically derived $K_p(q)$.

---

[c] Note that [30] finds evidence that the cloud density has $\alpha \approx 2$, $C_1 \approx 0.08$, however the results may be biased by the measuring device.

[d] Real radiances and cloud liquid water are nonstationary involving a third universal multifractal parameter H.

[e] Note that for large κ, the bound $q<1$ is equivalent to $\gamma < C_1$, $\gamma_p > -C_1/(1-C_1)$.

4. RENORMALIZATION

We can now relate the transmission statistics of lognormal multifractal clouds to those of a homogeneous cloud. At first sight this seems to be a difficult task since we already explained in the introduction that in the thick limit (κ large) both types of clouds will result in a completely different behavior of the radiative transfer properties. In this section however we will show that the photon statistics of a multifractal cloud can be approximated by the photon statistics of a "renormalized" homogeneous cloud in a certain range of photon singularities. In the following section we will relate this to multiple scattering and to results of diffusion on the same multifractals.

We seek to replace the multifractal cloud with a nearly equivalent homogeneous cloud with "effective" extinction coefficient $\kappa_{eff}=\kappa^{a}$. This cloud has the direct transmission given by $T(x)=e^{-\kappa_{eff}x}$ which leads to the following linear $K_p(q_p)$:

$$K_{p,hom}(q_p)=q_p-aq_p \tag{29}$$

A linear $K_p(q_p)$ therefore indicates exponential transmission T(x) (note that the Legendre transformation breaks down in this case so that there is no corresponding $c_p(\gamma_p)$). Now we compare this with the $K_p(q_p)$ for a multifractal cloud. Using the fact that in the large k limit, the scattering is dominated by $q_p=q=0$, we obtain to leading order:

$$a=\lim_{q_p\to 0}\frac{K_p(q_p)-q_p}{q_p}=1-\gamma_p(q_p=0)=\frac{1}{1-K'(0)} \tag{30}$$

The linear approximation $K_p(q_p)\approx q_p-q_p a$ leads to a renormalized extinction coefficient of the homogeneous cloud (using $K'(0)=-C_1$ for $\alpha=2$):

$$\kappa_{eff}=\kappa^{\frac{1}{1+C_1}} \tag{31}$$

The linearity of the $K_p(q_p)$ function, hence accuracy of the approximation in the range q_p is quite high (see for example fig. 5).

4.2. COMPARISON WITH MULTIPLE SCATTERING SIMULATIONS:

For lognormal multifractals, it is not difficult to extend the above single scattering results to the multiple scattering case, the main difficulty being the adequate treatment of the correlation structure. This treatment (developed elsewhere) does indeed confirm that correlations play only a secondary role in the large κ limit, as suggested by the near linearity of K_p.

In order to test this idea, we considered the numerical transmission results on lognormal multifractal clouds (with $C_1=0.5$) published in [15, 16] (see Fig. 6). These simulations were made using two dimensional discrete lognormal cascades with scale ratio factor 2 per step, total range of scales 2^{10}. Cyclic boundary conditions were used in the horizontal and photons were vertically incident. Isotropic discrete angle phase functions were used and the resulting fields in each of the four directions at 90^{o}, as well as the overall albedo and transmission were calculated by both Monte Carlo and relaxation techniques (the agreement of the two methods increased confidence in the results). The extinction coefficient was increased by factors of two so that the total mean optical thickness $\kappa\langle\rho\rangle$ increased from 12.5 to 200. In order to obtain the theoretically predicted renormalization result, we recall that for plane parallel clouds, with the same boundary conditions and the Discrete Angle (2,4) Radiative Transfer phase functions [8], $1+\frac{1}{2}(1-t+r)\kappa$ where t, r are the discrete angle forward and backward scattering coefficients respectively. In [15] isotropic DA phase functions were used (i.e. t=r=1/2). Using this result and the effective extinction coefficient in place of the true optical thickness $\tau=\kappa_{eff}<\rho>=\kappa_{eff}$, we obtain:

$$\langle T\rangle=\frac{1}{1+\frac{1}{2}\kappa^{\frac{1}{1+C_1}}}\approx 2\kappa^{-\frac{1}{1+C_1}} \tag{32}$$

Fig. 6 shows the result of superposing this function on the numerics, which are nearly power law even for κ as low as 12.5. The total transmittances through the renormalized homogeneous cloud show for all values of κ only less than 20% difference from the total transmittances through the multifractal cloud. Closer examination shows that there is a slight curvature suggesting that there are still some residual small κ effects and that a better estimate might be obtained by considering only the last two points. Indeed, this is remarkably close to the theoretical renormalization result (a=2/3) since it yields $a\approx0.65$. These results suggest that renormalization will give accurate results for bulk transport properties in multifractal systems with other boundary conditions, perhaps even with modest optical thicknesses.

4.3 COMPARISON WITH DIFFUSION:

The surprisingly accurate prediction of reference [15] thick cloud numerics can perhaps best be understood by considering the relation between radiative transfer and diffusion on multifractals. In general, there will be two significant limits: the large Λ (wide cascade range) and large κ (thick cloud) limits. Clearly, for fixed and finite Λ, if the cloud is made thick enough, ($\kappa>>\Lambda$) the mean free path will be much smaller than a single resolution element and the photons will diffuse through each homogeneous region of size Λ^{-1}. The overall result will be photons diffusing through the multifractal cloud. In actual fact, diffusion can still occur under somewhat less stringent conditions when κ is large, the main requirement being that weak density regions become so rare that direct photon transmittance across a large fraction of the cloud is statistically negligeable. The multifractals with $\alpha<2$ have precisely the property that they are dominated by weak events (negative singularities) called "Levy holes". It is a priori possible that -even with large κ- if Λ is sufficiently large (the order of the limits $\Lambda\to\infty$ and $\kappa\to\infty$ is important i.e. with κ fixed, but with $\Lambda \to \infty$) they will have large regions dominated by the holes, and hence lead to nondiffusive transfer.

However, in the case studied here, the parabolic shape of $c(\gamma)$ guarantees that large negative γ's and the corresponding weak regions are extremely rare, indeed, in the preceeding development, we have seen that the value of Λ is essentially irrelevant as long as it is sufficiently large. We therefore anticipate that the photons will diffuse for large enough κ. To make this plausible, we cite a recent analytic result believed to be exact for diffusion in one dimensional log-normal multifractals [35]:

$$\left\langle x^2 \right\rangle \propto t^{\frac{1}{1+C_1}} \tag{33}$$

for the RMS particle distance after time t in a lognormal multifractal with codimension of the mean=C_1. Noting that normal diffusion has linear variance growth, we can make the identification between the multifractal distance above and an equivalent homogeneous "effective" distance:

$$\left\langle x^2 \right\rangle^{\frac{1}{1+C_1}} \approx \left\langle x^2 \right\rangle_{eff} \tag{34}$$

Finally, identifying the mean free path $\kappa^{-1}= <x^2>^{1/2}$, we obtain:

$$\kappa^{\frac{1}{1+C_1}} \approx \kappa_{eff} \tag{35}$$

The above multiple scattering arguments are therefore completely consistent with the diffusion results. Note that for diffusion in spaces with dimensions higher than one, the above diffusion result is no longer exact, whereas our scattering arguments appear to be valid in a space of any dimension.

5. CONCLUSIONS:

We have developed a formalism analogous to the multifractal singularity formalism for understanding photon scattering statistics in radiative transfer in multifractal media, and have tested the results numerically on lognormal multifractals. Although the results are only exactly valid in the thick cloud limit, the approximation was found to be quite accurate down to $\kappa\approx1$-10, so that the results may be widely applicable. The theory involved two fundamental quantities: the photon path exponent scaling function $K_p(q_p)$ for moments order q_p, and the analogue codimension function $c_p(\gamma_p)$ that determines the scattering probabilities for various nondimensional path distances $\tau_p=\kappa x=\kappa^{\gamma_p}$.

It was shown that the near linearity of $K_p(q_p)$ lead to the possiblity of "renormalizing" the multifractal by replacing it with a near equivalent homogeneous medium but with an effective extinction coefficient $\kappa^{1/(1+C_1)}$ where C_1 is the codimension of the mean singularity of the cloud. Finally, we argued that this approximation was likely to continue to be valid for multiple scattering, and was also compatible with recent results for diffusion on lognormal multifractals. We compared our results with recent numerical calculations finding excellent agreement.

The main limitation of these results is their restriction to the cases where $K(q)$ is analytic at $q=0$ (i.e. for universal multifractals, $\alpha=2$), whereas empirical results indicate $\alpha\approx1.35$ is more accurate for radiation in real clouds). The key point in the development is the approximation of the bare multifractal properties by the dressed ones; when $\alpha<2$, this step is still straightforward for the larger singularities, but may breakdown for the regularities associated with the numerous weak "Levy hole" events that will dominate the scattering. However, preliminary numerics indicate that even here, similar treatment may be possible using appropriate asymptotic dressed multifractal properties. This -as well as extensions to full multiple scattering statistics - is an important area for future work.

6. REFERENCES

1. Korvin, G., 1992, "Fractal models in earth Sciences", *Elsevier*, 396pp.
2. Scholz C. H.and B. B. Mandelbrot, 1989, "Fractals in geophysics", *Birkhäuser*.
3. Schertzer, D. and S. Lovejoy, 1991, *Non-linear variability in Geophysics; scaling and fractals*. Kluwer, Schertzer, D., and Lovejoy S., pp. 41-82.
4. Lam, N. S.-N., L. de Cola, 1993, "Fractals in Geography", *PTR Prentice Hall*.

5. Gabriel, P., S. Lovejoy, G.L. Austin, and D. Schertzer, 1986, "Radiative transfer in extremely variable fractal clouds", paper presented at the *6th Conference on Atmospheric Radiation*, Am. Meteorol. Soc., Williamsburg, Va., May 12-16.
6. Adams, M., L. Adams, E. W. Larsen, G. C. Pomeraning, 1989: Benchmarck results for particle transport in a minary markov statistical medium, *J. Quant. Spec. and Rad. Trans.*, **42**, 253.
7. Lovejoy, S., P. Gabriel, D. Schertzer, and G.L. Austin, 1988, "Fractal Clouds With Discrete Angle Radiative Transfer", *IRS proceedings*, pp. 99-102.
8. Lovejoy, S., A. Davis, P. Gabriel, D. Schertzer, G. L. Austin, 1990, "Discrete Angle Radiative Transfer - Part I: Scaling and Similarity, Universality and Diffusion", *Geophys. Res.*, **95**, 11699-11715.
9. Davis, A., P. Gabriel, S. Lovejoy, D. Schertzer, 1988, "Scaling Laws For Asymptotically Thick Clouds, Dimensional Dependence - Phase Function Independence", *IRS proceedings*, pp. 103-106.
10. Davis, A., P. Gabriel, S. Lovejoy, D. Schertzer, G. L. Austin, 1990, " Numerical Results And Meteorological Applications", *Geophys. Res.*, **95**, 11729-11742.
11. Gabriel, P., S. Lovejoy, A. Davies, D. Schertzer, G. L. Austin, 1990, "Renormalization Approach For Homogeneous And Fractal Clouds", *Geophys. Res.*, **95**, 11717-11728..
12. Cahalan, R. F., 1989, "Overview of Fractal Clouds", paper presented at RSRM'87, *Advances in Remote Sensing*, pp 371-389, edited by A. Deepak et al., A. Deepak, Hampton, Va.
13. Barker H. W. and J. A. Davies, 1992, "Solar Radiative Fluxes for Stochastic, Scale-invariant Broken Cloud Fields", *J. Atmos. Sciences*, **49**, 1115-1126.
14. Evans, K. F., 1993, "A General Solution For Stochastic Radiative Transfer", *G.R.L.*, **20**, 19, pp. 2075-2078.
15. Davis, A., S. Lovejoy, D. Schertzer, 1991, "Discrete angle radiative transfer in a multifractal medium", *SPIE-Proceedings*, vol. 1558, pp 37-59.
16. Davis, A., S. Lovejoy, D. Schertzer, 1993, "Supercomputer Simulation Of Radiative Transfer In Multifractal Cloud Models", *IRS-Proceedings*, pp 112-115.
17. Novikov, E. A. and Stewart, 1964, "Intermittency of turbulence and spectrum of fluctuations in energy-dissipation", *Izv. Akad. Nauk. SSSR. Ser. Geofiz*, **3**, 408-412.
18. Kolmogorov, A. N., 1962, "A refinement of previous hypothesis concerning the local structure of turbulence in viscous incompressible fluid at high Raynolds number", *J. Fluid Mech.*, **83**, 349.
19. Obukhov, A., 1962, "Some specific features of atmospheric turbulence", *J. Geophys. Res.*, **67**, 3011.
20. Yaglom, A. M., 1966, "The influence on the fluctuation in energy dissipation on the shape of turbulent characteristics in the inertial interval", *Sov. Phys. Dokl.*, **2**, 26-30.
21. Mandelbrot, B. B. , 1974, "Intermittent turbulence in self-similar cascades: divergence of high moments and dimension of the carrier", *J. Fluid Mech.*, **62**, 331-350.
22. Frisch, U., P. L. Sulem, and M. Nelkin, 1978, "A simple dynamical model of intermittency in fully developed turbulence", *J. Fluid Mech.*, **87**, 719-724.
23. Schertzer D., and S. Lovejoy, 1983, "Elliptical turbulence in the atmosphere", in *proceedings of the fourth symposium on turbulent shear flows 11.1-11.8*, Karlsruhe, West Germany.
24. Benzi, R., G. Paladin, G. Parisi, and A. Vulpiani, 1984, "On the multifractal nature of fully developed turbulence", *J. Phys.. A.*, **17**, 3521-3531.
25. Meneveau, C. and K. R. Sreenevasan, 1987, "Simple multifractal cascade model for fully developed turbulence", *Phys. Rev. Lett.*, **59**, 1424-1427.
26. Schertzer, D. and S. Lovejoy, 1987, "Singularités anysotrope, divergence des moments en turbulence", *Ann. Sc. math. du Québec*, **11**, 1, 139-181.
27. Schertzer, D. and S. Lovejoy, 1987, "Physical modeling and Analysis of Rain and Clouds by Anisotropic Scaling of Multiplicative Processes", *J. Geophys. Res.*, **92**, 8, 9693-9714.
28. Parisi, G., and U. Frisch, 1985, "A multifractal model of intermittency", in *turbulence and predictability in geophysical fluid dynamics*, North Holland, Ghil, M., R. Benzi, and G. Parisi, pp. 111-144.
29. Lovejoy, S., B. Watson, D. Scherzter, G. Brosamlen, 1994: Scattering in universal multifractals, Physica A, in preparation.
30. Brosamlen, G., 1994: Radiative transfer in lognormal multifractal clouds and analysis of cloud liquid water data, MSc. thesis, McGill University, 69pp.
31. Schertzer, D., S. Lovejoy, 1994: Multifractal Generation of Self-Organized Criticality, in *Fractals In the natural and applied sciences* Ed. M.M. Novak, Elsevier, North-Holland, 325-339.
32. Tessier, I., S. Lovejoy, and D. Schertzer, 1993, Universal Multifractals: Theory and Observations for Rain and Clouds, *J. Appl. Meteorology*, **32**, 223-250.
33. Lavallée, D., 1991, "Multifractal techniques: Analysis and simulation of turbulent fields", Ph.D. thesis, McGill University, Montréal, Québec, Canada.

34. Lavallée, D., S. Lovejoy, and D. Schertzer, 1991, "On the determination of the codimension function", in *Non-linear variability in geophysics: Scaling and fractals*, Kluwer, Schertzer, D. and S. Lovejoy, pp. 99-110.
35. Silas, P., 1994, M.Sc. Thesis, McGill University, Montréal (Québec), Canada.
36. Lovejoy, S., D. Schertzer, B. Watson, 1992: Radiative Transfer and Multifractal Clouds: theory and applications, *Inter. Rad.Sympos.. 92*, A. Arkin et al Eds. 108-111.

<u>Figure Captions:</u>

<u>Figure 1</u> Photon "random walk" in a multifractal cloud (C_1= 0.1; Λ=512) with extinction coefficient κ=32 in a) and κ=128 in b). The y-axis represents the cloud density ρ and the number of scatters of the photon (1 unit corresponds to 20 scatters). The x-axis represents the position in the 1-d cloud. Clearly to see is that with increasing extinction coefficient κthe mean free path length of the photon decreases.

<u>Figure 2:</u> PDMS analysis of the free-photon path length probability distribution. Simulation with α=2, C_1=0.1 , scale of homogeneity Λ=4096, 1000 realizations, 512 photon-starting points in each realization. The upper 4 lines represent $\log Pr(\tau_p < \kappa^{\cdot\cdot r})$ whereas the lower 4 lines represent $[\log Pr(\tau_p > \kappa^{\cdot\cdot r})] - 1$. The scaling holds down until κ=8. For γ_p=-0.5 and γ_p=0.6 the scaling is not provided anymore which is in good agreement with the of theoretically predicted limits ($\gamma_p^{\cdots} = -0.33$, $\gamma_p^{\cdots} \approx 0.6$).

<u>Figure 3:</u> Comparison of the analytically derived bare $c_p(\gamma_p)$-function with the numerically derived $c_{p,d}(\gamma_p)$-function obtained from the slopes in the previous graph (in the range 8<κ<256). In the predicted range of validity $\gamma_p^{\cdots} = -0.33 < \gamma_p < 0.6 = \gamma_p^{\cdots}$ there is a good agreement between both curves. The left branch represents $Pr(\tau_p < \kappa')$ and the right branch represents $Pr(\tau_p > \kappa')$.

<u>Figure 4:</u> Scaling of the moments of the dressed photon path length τ_p as a function of κ.. $\log < \tau_p^q >$ versus logκ for various values of q. There is a very good scaling for κ>8 since the lines are straight in that regime. The scaling breaks down for smaller κ since a unique normalization is not provided anymore. Data from simulation with α=2, C_1=0.1, 4096 realizations, 512 photons/realization.

<u>Figure 5:</u> Comparison of the moment scaling exponent function $K_p(q)$ for the "bare" with $K_{p,d}(q)$ for the "dressed" photon path length for a field α=2, C_1=0.1. In the range -0.5 < q < 6 both curves are in very good agreement. The dressed $K_{p,d}(q_p)$ curve was obtained from the simulation with 4096 realizations, 512 photons/realization.

<u>Figure 6:</u> Result on total transmission after multiple scattering through 2-d multifractal cloud (C_1 =0.5) published in [15] compared to the thick cloud limit of the transmission through a homogeneous cloud with renormalized extinction coefficient κ_{eff}.

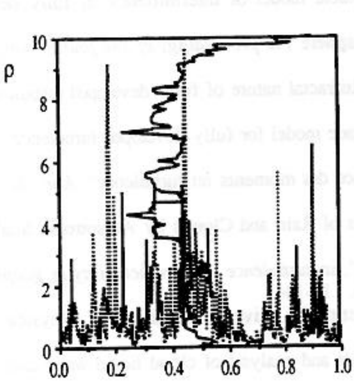

<u>Figure 1</u>

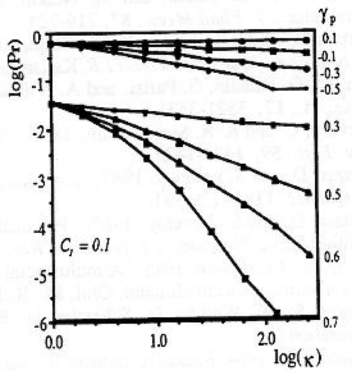

<u>Figure 2:</u>

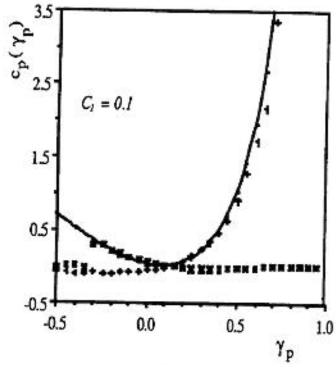

Figure 3:

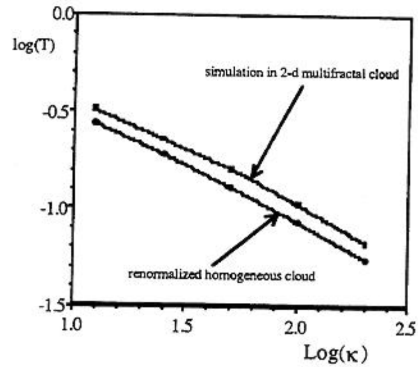

Figure 6:

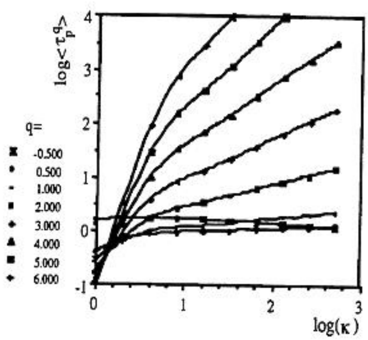

Figure 4:

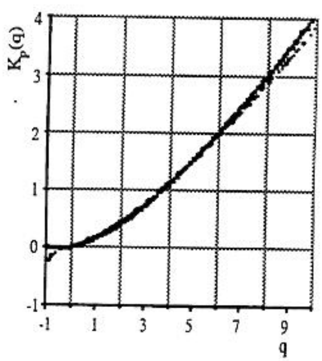

Figure 5: